Comprehensive Journal of Science
Volume (9), Issue (36), (Sept 2025)
ISSN: 3014-6266

مجلة العلوم الشاملة
المجلد(9) العدد (36) (سبتمبر 2025)
ردمد: 3014-6266

Aerodynamic Analysis of Darrieus Wind Turbine Using Blade Element Theory

Basim Al Tlua1, Adil Aledresse2, Akram Halap3and Mohsen Asheni 4
1,2,3,4Libyan Center for Land and Marine Environmental Research (LCLMER), Zwara, Libya
altlua.basim@gmail.com

التحليل الهيدروديناميكى لتوربينة الرياح داريوس باستخدام نظرية عنصر الشفرة

محسن عشينى و [3]اكرم حلب [2] ,عادل الادريسى [1],باسم التلوع [4]
المركز الليبي لبحوث البيئة البرية والبحرية, زواره- ليبيا [1,2,3,4]

Received: 5-09-2025; Revised: 10-09-2025; Accepted: 15-09-2025; Published 30 -09-2025

Abstract:
This document presents a detailed analysis of the application of Blade Element Theory (BET) to a Darrieus wind turbine design, featuring two Troposkien blade shapes, each incorporating a constant symmetrical NACA0015 airfoil. BET is a widely used method for analyzing the aerodynamic performance of wind turbine blades and for aiding the design process. The study calculates the aerodynamic blade loads by evaluating forces on individual blade elements and integrates these results to estimate the overall performance. These calculated results, specifically the torque coefficient and power coefficient, are compared to available experimental data, revealing that the theoretical predictions show reasonable agreement, albeit with some discrepancies. These differences are likely attributable to the simplifications in the BET model, such as the neglect of vortex effects, which can influence the accuracy of results under certain conditions. Despite these limitations, the BET method provides a practical tool for wind turbine designers, offering a useful balance between computational efficiency and performance estimation. However, it is acknowledged that BET is not ideal for accurately simulating the wake effects or capturing the complexities of three-dimensional flow phenomena. The study concludes that while BET is effective for preliminary design and analysis, further research and more advanced simulations are necessary to refine the methodology and improve the precision of wind turbine performance predictions.
Keywords: Darrieus wind turbine; vertical axis wind turbine; blade element theory.

الملخص:
تقدم هذه الورقة تحليلًا مفصلاً لتطبيق نظرية عنصر الشفرة (BET) في تصميم توربينة هوائية من نوع داريوس، الذي تتميز بشكلين من اجنحة التروبوسكين، حيث يتضمن كل منهما جناح هوائي ثابت المقطع متماثل من نوع NACA0015. تُعد نظرية عنصر الشفرة طريقة مستخدمة على نطاق واسع لتحليل الأداء الهيدروديناميكي لأجنحة التوربينات الهوائية والمساعدة في عملية التصميم. الدراسة تشمل حساب الأحمال الهيدروديناميكية على الأجنحة من خلال تقييم القوى المؤثرة على كل مقطع على حدى ودمج هذه النتائج لتقديرالأداء العام للتوربينة الهوائية. تتم مقارنة النتائج المحسوبة، والتي تشمل معامل العزم ومعامل القدرة، مع البيانات التجريبية المتاحة، مما يكشف أن التنبؤات النظرية تظهر توافقًا جيدا ، وعلى الرغم من وجود بعض الاختلافات والتي من المحتمل أن تعزى إلى التبسيطات في نموذج BET ، مثل إهمال تأثيرات الدوامات، التي يمكن أن تؤثر على دقة النتائج في ظل بعض الظروف وعلى الرغم من هذه القيود، تعتبر طريقة BET أداة عملية لمصممي التوربينات الهوائية ، حيث تقدم توازنًا مفيدًا بين الكفاءة الحسابية وتقدير الأداء . ومع ذلك، تعتبر BET ليست دقيقة في محاكاة تأثيرات الاضطراب أو لتمثيل التعقيدات الموجودة في الجريان ثلاثي الأبعاد. وتخلص الدراسة إلى أنه في حين أن BET فعالة للتصميم والتحليل الأولي، إلا أن المزيد من البحث والمحاكاة المتقدمة ضرورية لتحسين المنهجية وتحسين دقة التنبؤات المتعلقة بأداء التوربينات الهوائية.
الكلمات الدالة: توربينات الرياح داريوس؛ توربينات الرياح ذات المحور الرأسي؛ نظرية عنصر الشفرات.

Introduction

Wind energy is an attractive alternative source of energy. Statistics from the united state have shown growing prospects for installation and usage of wind power generation [1]. Wind turbines convert kinetic energy from the wind into mechanical energy, which is used to generate electricity.

Today's wind turbines are manufactured in a range of vertical and horizontal axis types. The horizontal axis wind turbine is the most common turbine configuration. The turbine mechanisms are mounted high above the ground on a tall pedestal. It is a matter of opinion as to whether they enhance the landscape. However, there is no denying that the height at which their mechanisms are located is a disadvantage when servicing is required. Also, they require a mechanical yaw system to orient them

such that their horizontal axis is perpendicular to and facing the wind. As potential power generation is related to the swept area (diameter) of the rotor, more power requires a larger diameter. The blades experience large normal and tangential forces, so size is limited by blade strength. Larger wind turbines are more efficient and cost-effective.

A vertical-axis wind turbine does not need to be oriented into the wind and the power transition mechanisms can be mounted at ground level for easy access. The perceived disadvantage of VAWT is that they are not self-starting. However, it could be argued that HAWT is also not self-starting since it requires a yaw mechanism for orientation. Currently, VAWTs are usually rotated automatically until they reach the ratio between blade speed and undisturbed wind speed (Tip Speed Ratio or TSR) that produces a torque large enough to do useful work. Through the use of drag devices and/or variable pitch blade designs, it is hoped that a VAWT will be able to reach the required TSR without the use of a starter.

To design a wind turbine, an analysis tool is needed for performance predictions of designed wind turbines. Almost all wind turbine design tools use Blade Element Theory (BET) for aerodynamic analysis. BET is very fast, computationally speaking and gives good results for steady-state conditions [2].

Vertical Axis Wind Turbine

There are two distinct types of vertical axis wind turbine: The Savonius and the Darrieus type Figure (1). The Darrieus rotor was researched and developed extensively by Sandia National Laboratories in the 1980's. Over the past two decades, the Darrieus-type vertical-axis wind turbine (VAWT) has undergone considerable research and significant engineering development.

The vertical axis wind turbines (VAWT) have been receiving an increased acceptance for urban wind turbine integration in the future smart grid [3]. The VAWT has several advantages over the more conventional horizontal axis wind turbines (HAWT): The smaller number of components; low sound emissions; their sensitivity to fast changes in wind flow direction; a lower architectural visual impact; the ability to operate closer to the ground; and others. However, the VAWT aerodynamic performance is more complex to simulate and predict due to its operation.

(a) (b)

Figure 1: a) Savonius VAWT, and b) Troposkien-Darrieus VAWT.

Aerodynamics Of Vawts

The first aerodynamic vertical axis wind turbine was developed by Georges Darrieus in France and first patented in 1927. Its principle of operation depends on the fact that its blade speed is a multiple of the wind speed, resulting in an apparent wind throughout the whole revolution coming in as a head wind with only a limited variation in angle [3].

3.1 Single Stream Tube Model

The first model to calculate the aerodynamic performance of a curved-blade vertical-axis wind turbine Figure (2) was by Templin [4] and the model was called the Single Stream tube Model. This model

assumes a velocity to be constant through the blades and related directly to wind turbine drag. The induced velocity is assumed to be the same through two faces of the rotor, upwind and downwind. According to Glauert's theory [5] the wind turbine drag is given by

$$D = 0.5\,\rho\,S\,U_b\,(U_w - U_b) \quad (1)$$

Where:

U_b is the velocity through the blades.

U_w is wind velocity

ρ represents the fluid density

S is the surface area

A blade drag coefficient C_{bd} is based on dynamic pressure and the blade area is defined as:

$$C_{bd} = \frac{D}{0.\rho\,U_b^2\,S} \quad (2)$$

And from equation (1)

$$C_{bd} = 4\,[\frac{U_w}{U_b} - 1] \quad (3)$$

Hence

$$\frac{U_w}{U_b} = 1 + 0.25\,C_{bd} \quad (4)$$

For structural design, a convenient drag coefficient Cbd is based on ambient dynamic pressure, where;

$$C_{bd} = \frac{D}{0.5\,\rho\,U_w^2\,S} = C_{bd}\,[\frac{U_b}{U_w}]^2 = \frac{C_{bd}}{[1 + 0.5\,C_{bd}]^2} \quad (5)$$

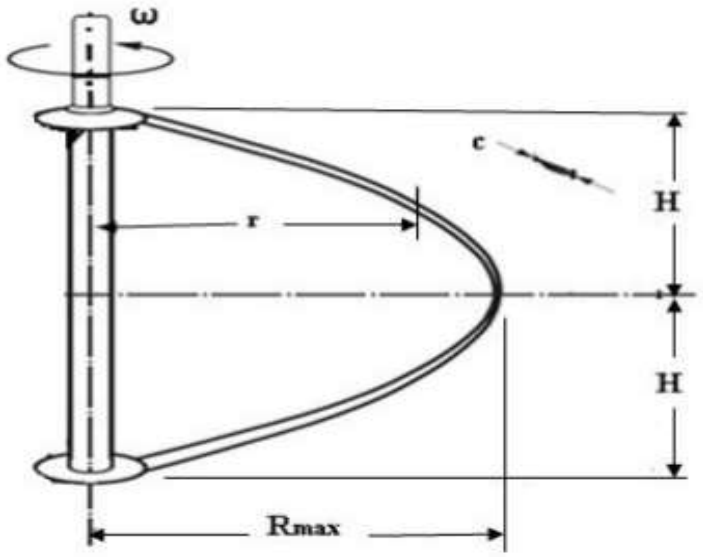

Figure 2: carved blade vertical axis wind turbine.

For a given wind turbine geometry and rotational speed, the aerodynamic performance, turbine power and rotor drag are calculated using the blade element theory.

3.2 Blade Element Theory

The blade element theory provides sufficient information for detailed design. Detailed information can be obtained through analysis of the forces acting on the blade element. These forces act on small sections of the blade. A differential blade element of chord c and width dr located at radius r from the hub is shown in Figure (3).

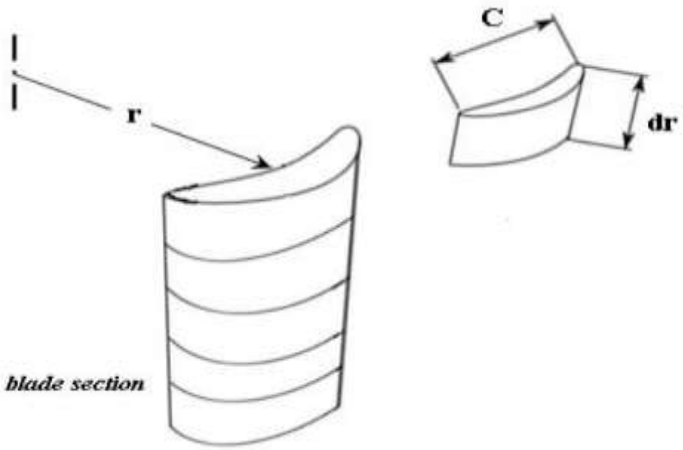

Figure 3: Schematic of blade elements.

The force on the blades of a wind turbine can be expressed as a function of lift and drag coefficient and angle of attack, as shown in Figure (4), for this analysis, the blade is assumed to be divided into N sections or elements. The following assumptions are made:

- There is no aerodynamic interaction between elements.
- Lift and Drag forces are determined solely by the characteristics of the airfoil shape of the blade.

To analyze the force on the blade section, it must be considered that the lift and drag are perpendicular and parallel, respectively, to an effective wind.

Relative Flow

The lift and drag coefficient data are available for a variety of airfoils from wind tunnel data. Since most wind tunnel testing is done with the airfoil stationery, available in the literature the flow over the moving airfoil has to be connected to that of the stationary test, so that the relative velocity over the airfoil is used. Let U_w be an absolute wind speed, Urel its relative speed and U_b the blade velocity,

$$U_b = \Omega r \qquad (6)$$

It results

$$U_{rel} = U_w - U_b = U_w - \Omega r \qquad (7)$$

Where:

Ω – turbine rotor angular velocity

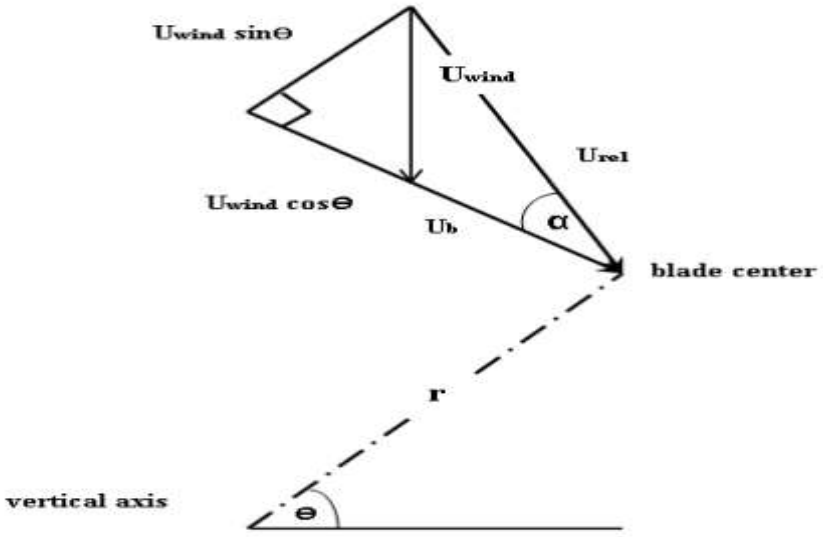

Figure 4: blade element characteristics velocities.

On Figure (4) the relative velocity components along the specified axes are

$$U_s = U_b + U_w \cos\Theta \qquad (8)$$

The U_n normal component (perpendicular to the gust element) of the U_{rel}:

$$U_n = U_w \sin \Theta \quad (10)$$

To calculate the aerodynamic forces acting on the blade element the component of the relative wind speed shall be considered

$$U_{rel}^2 = U_s^2 + U_n^2 \quad (11)$$

The following relation is obtained

$$U_{rel}^2 = (\Omega r + U_w \cos \Theta)^2 + (U_w \sin \Theta)^2 \quad (12)$$

For (α) angle of attack, defined by the relation

$$tan(\alpha) = \frac{U_n}{U_S} \quad (13)$$

It results

$$tan(\alpha) = \frac{U_w \sin(\alpha)}{[\Omega r + U_w \cos(\alpha)]} \quad (14)$$

The local Tip-Speed Ratio (TSR) is defined as:

$$TSR = \frac{\Omega r}{U_w} \quad (15)$$

Blade Elements

The forces that act on the blade element are shown in Figure (10). The lift and drag forces are perpendicular and parallel to the incoming flow. For each blade element:

$$C_n = C_L \cos(\alpha) + C_D \sin(\alpha) \quad (16)$$

$$C_t = C_L \sin(\alpha) - C_D \cos(\alpha) \quad (17)$$

Where:

C_n – normal aerodynamic coefficient,

C_t – tangential aerodynamic coefficient,

C_L – lift coefficient

C_D – drag coefficient

The angle of attack (α) varies over a complete rotation of considered blade element, being dependent on the azimuthal angle (Θ).

The element's normal force (N) and the tangential force (T) acting on the blade element depends on the coefficient C_n and C_t

$$N = q\, C_n\, c\, dr \quad (18)$$

$$T = q\, C_t\, c\, dr \quad (19)$$

Where:

q- represents the dynamic pressure

$$q = 0.5\, \rho\, U_b^2 \quad (20)$$

The lift and drag coefficient for a NACA0015 airfoil are shown in Figure (5).

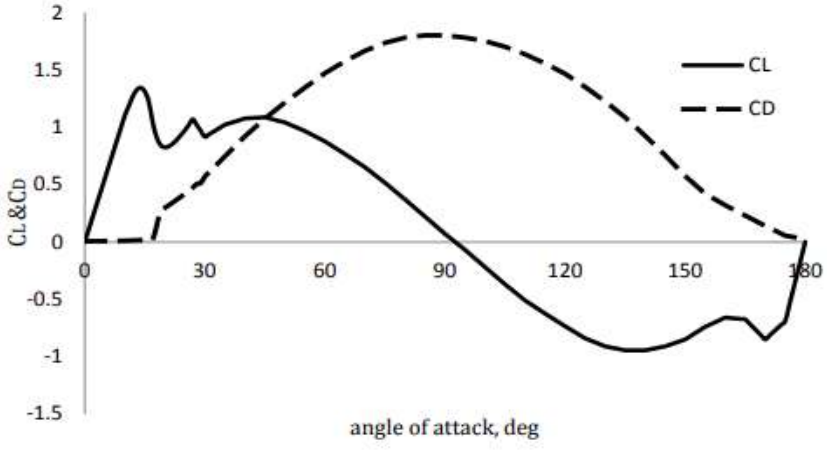

Figure 5: lift and drag coefficient for NACA0015 airfoil.

The graph above shows that for low values of angle of attack; the airfoil produces a large amount of lift with little drag. At around 15 deg angle of attack, a stall occurs where there is a massive increase in drag and a sharp reduction in lift. If there are B blades combining Equations (16), (17) and Equations (18), (19), (20) it can be shown that:

$$N = B\,0.5\,\rho\,U_b^2\,(C_L \sin(\alpha) - C_D \cos(\alpha))\,cdr \qquad (21)$$

$$T = B\,0.5\,\rho\,U_b^2\,(C_L \cos(\alpha) + C_D \sin(\alpha))\,cdr \qquad (22)$$

The elemental torque due to the tangential forces, (T) operating at a distance, (r) from the hub is given by

$$Q = T\,r \qquad (23)$$

Hence the elemental torque by inserting equation (22) into equation (23)

$$Q = B\,0.5\,\rho\,U_b^2\,(C_L \cos(\alpha) - C_D \sin(\alpha))c\,r\,dr \qquad (24)$$

The effect of drag force is clearly seen in the equations, an increase in normal force on the machine will decrease in torque and power output.

These equations can be made more useful by substituting and carrying out some algebra yields:

$$N = Z\pi\rho U_b^2\,(C_L \sin(\alpha) + C_D \cos(\alpha))\,r\,dr \qquad (25)$$

$$T = Z\pi\rho U_b^2\,(C_L \cos(\alpha) - C_D \sin(\alpha))\,r^2 dr \qquad (26)$$

Where Z is called the local solidity and is defined as:

$$Z = \frac{B\,c}{2\pi\,r} \qquad (27)$$

Turbine Solidity As A Function Of Tsr

From tip-speed ratio, TSR the designer can determine the solidity, generator speed, and structural design of the rotor.

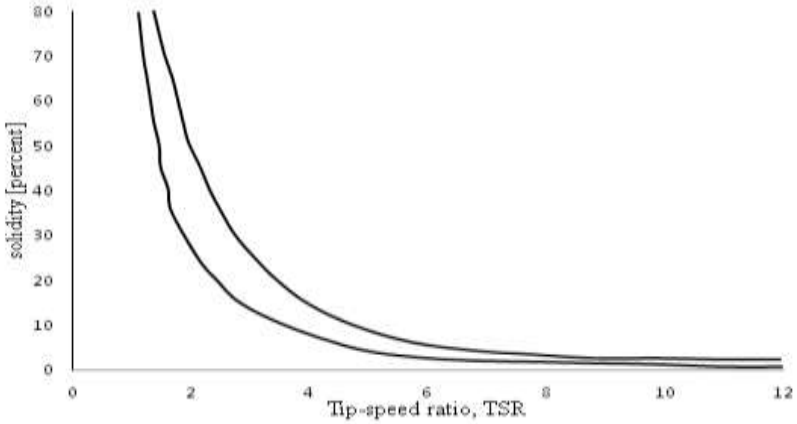

Figure 6: rotor solidity as a function of TSR [3]

Using TSR and the graph in Figure (6), a value of the solidity is selected then from the solidity the chord length can be found by: Solidity times the rotor frontal area gives the total blade area then dividing the total blade area, by the number of blades gives the individual blade area. Finally dividing the individual blade area by the rotor height gives the chord length [3].

Application Of The Blade Element Theory

7.1 Geometry Specification

Figure (7) shows the view of the 0.344 m-diameter model at Carleton University's low-speed wind tunnel test section. Two blades attached to the rotating tower were machined from ABS to NACA-0015 airfoil section and formed the curved shape. Each blade is made from four parts by using inner sleeve glue and screws. ABS filled surface was sanded to a fair 220-grit finish. The shape is a straight line/circular arc approximation of the Troposkien curve. The height of the turbine blades is 0.64 m with a maximum radius at the equator of 0.172.m.

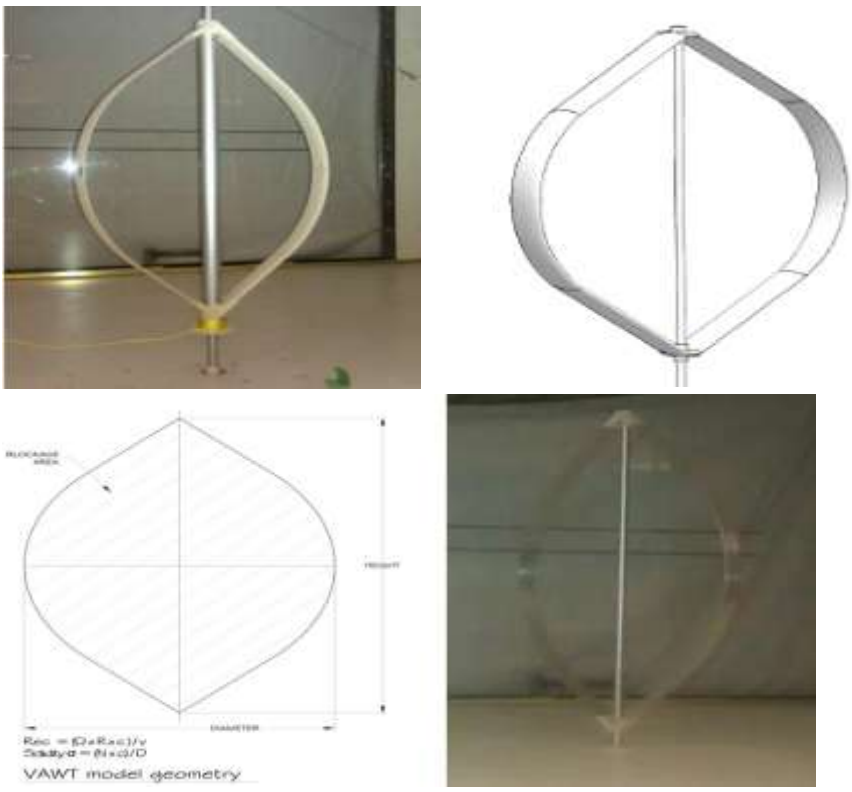

Figure 7: Carleton University VAWT wind tunnel test model [9].

7.2 GEOMETRY MEASUREMENTS:

The following details were specified about the geometry:

The height (m)	0.64
Equator diameter (m)	0.344
Height / Diameter (m)	1.5/1
Solidity	15%
Blockage area	9.3%
Number of blades	2
*Blade material	NBA
Blade section	NACA0015
Chord length (m)	0.038
Blade length (m)	0.64
Wind velocity (km/h)	48.5
Wind turbine rotation speed (rpm)	324

* ABS (from Carleton Rapid Prototype Machine)

Sections	*r(m)
0	0.0000
1	0.0117
2	0.0237
3	0.0351
4	0.0468
5	0.0585
6	0.0702

7	0.0819
8	0.0936
9	0.1053
10	0.1164
11	0.1265
12	0.1358
13	0.1441
14	0.1514
15	0.1576
16	0.1628
17	0.1668
18	0.1697
19	0.1714
r_{max} = 20	0.1720

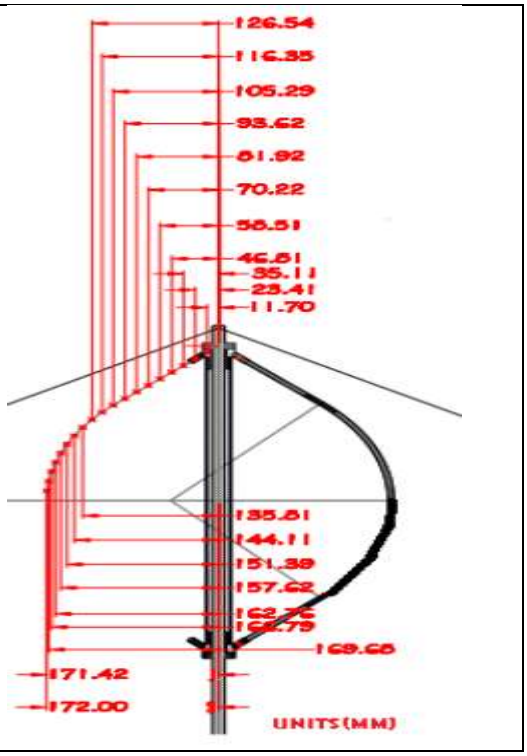

*r: Horizontal distance from the hub to the blade curve.

Figure 8: sections numbers for half blade and r for each section.

Procedure

This model describes a two-dimensional unsteady flow analysis around an airfoil in Darrieus motion under dynamic stall conditions (Figure 9). The aerodynamic model used here is based on the Blade Element Theory, which is the method being used in the current
report.

There are two forces of interest in this part of the study the tangential or torque force, s, and the normal force, n. Consider the actual blade divided into 40 finite elements with thickness, dr. The cross-section of the blade element looks like an airfoil, NACA0015, and can be analyzed as such. Here, the blade geometry is taken into consideration, and the torque and normal forces are evaluated for each element.

The first step to calculate these forces is to determine the velocity experienced by the blade element. Because the blade is rotating about the hub, each of the blade elements will experience a slightly different flow as they have a different rotational speed.

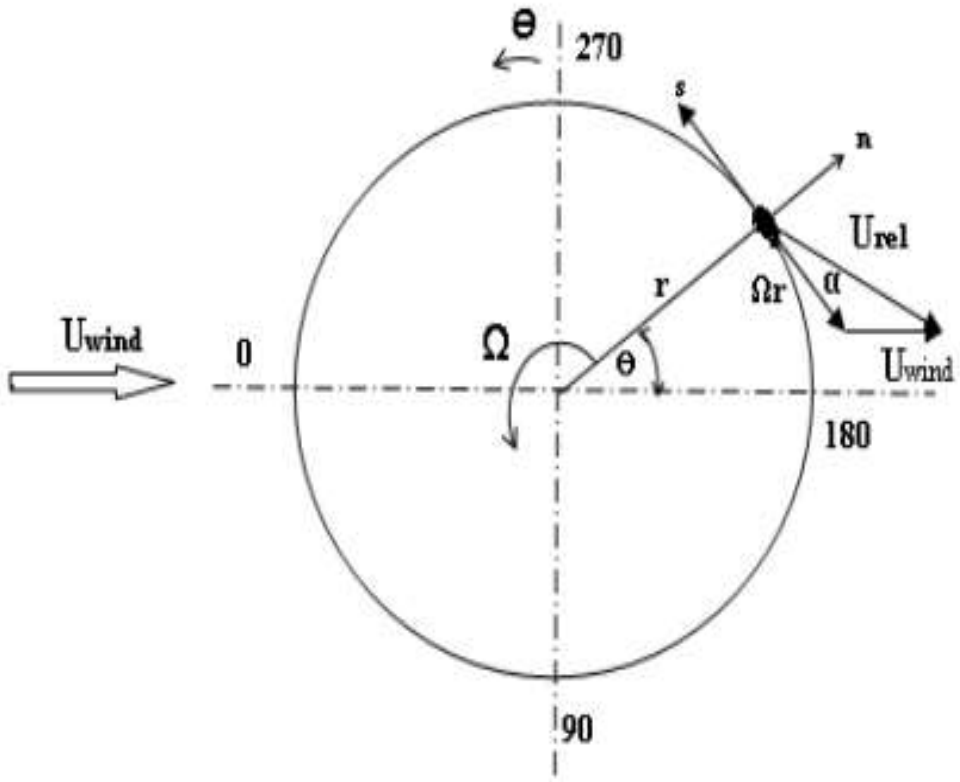

Figure 9: darrieus motion.

- Calculate the horizontal distance from the hub to the blade curve, r, then find out blade velocity U_b and relative velocity U_{rel}, where.

$$U_b = \Omega r$$

$$U_{rel}^2 = [\Omega r + U_w \cos(\Theta)]^2 + [U_w \sin(\Theta)]^2$$

- Calculate Reynolds number, Re, for each section $Re \ \frac{U_{rel}\, c}{\nu}$
- Calculate the angle of attack for each azimuthal angle and for all sections.

$$\alpha = actan\left[\frac{U_w \sin(\Theta)}{\Omega r + U_w \cos(\Theta)}\right]$$

- Finding C_L and C_D

From wind tunnel data, lift and drag coefficients are available for NACA0015 [7].

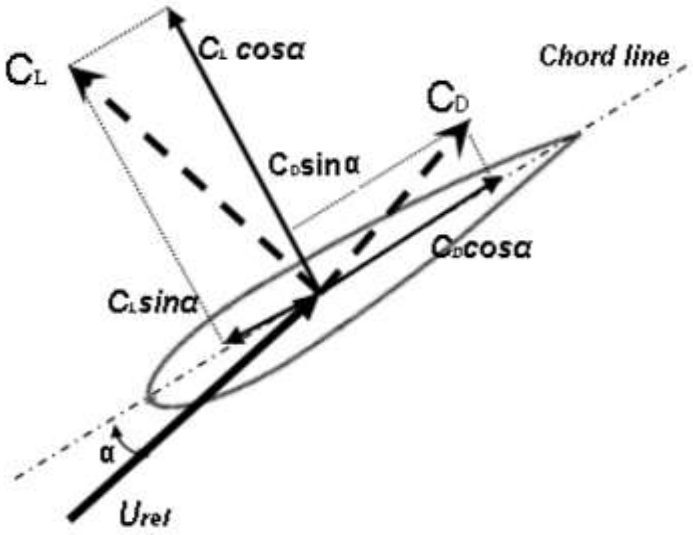

Figure 10: force coefficient of a blade element airfoil.

Calculate tangential coefficient force, C_t, and normal coefficient force, C_n.

$$C_n = C_L \sin(\alpha) + C_D \cos(\alpha)$$

$$Ct = C_L \cos(\alpha) - C_D \sin(\alpha)$$

The next step is to determine the lift and drag forces, which are functions of the angle of attack, α. The lift force turns the blade and acts perpendicular to U_{rel} and drags acts against lift and is parallel to U_{rel}. For a single blade, the final equations for these two forces at a blade element are:

$$N = 0.5\, C_N\, \rho\, U_b^2\, c\, dr$$

$$T = 0.5\, C_T\, \rho\, U_b^2\, c\, dr$$

From the last equation we can calculate the torque, Q. The Torque on an element is simply the tangential force, T, multiplied by the radius, r.

$$Q = 0.5\, C_T\, \rho\, U_b^2\, c\, r\, dr$$

The Torque coefficient, C_q, is defined as:

$$C_q = \frac{Q_{rotor}}{0.5\, \rho\, A_s\, R_{rotor}\, U_w^2)}$$

The Torque, Q, multiplied by the wind turbine rotating speed ω, it gives power.

$$P = Q\, \omega$$

The power coefficient is defined by

$$C_p = \frac{P}{0.5\, \rho\, A_s\, U_w^3}$$

Where: A_s is the rotor swept area.

Results And Discussion

The aerodynamic loads on Darrieus rotor blades were calculated using Matlab analysis based on the Blade Element Theory. In this model, lift and drag coefficients are taken from static airfoil data. The Darrieus rotor used a NACA0015 symmetrical airfoil with a constant chord along the entire length of the blade. The Darrieus rotor used a NACA0015 symmetrical airfoil with a constant chord along the entire length of the blade.

Figure (11) illustrates the C_L vs. (α) measurements at different Reynolds numbers and those given in reference [8]. A large difference may be noted between lift coefficients in the static-stall zone. After this region, C_L values increase and C_{Lmax} becomes greater than 1. The drag coefficient C_D as a function of an angle of attack (α) is plotted in Figure (12). The experimental data shows a C_{Dmax} of 1.8 at an incidence angle of 90 deg

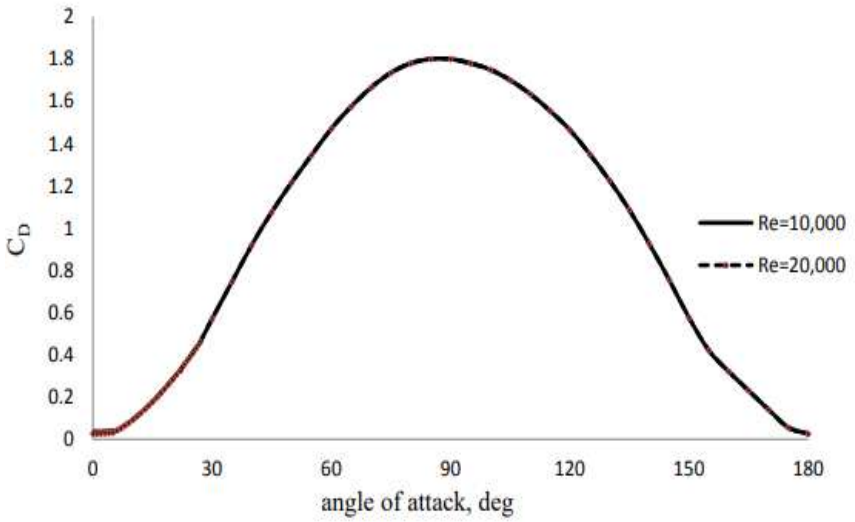

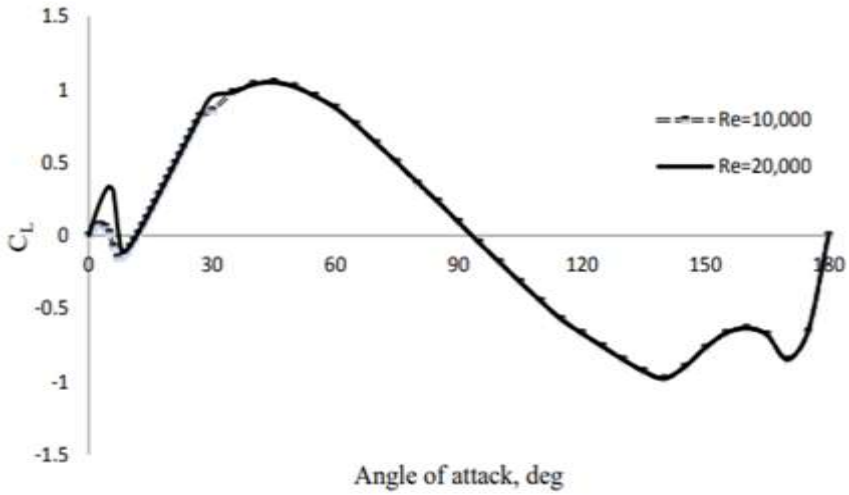

Figure 11: lift coefficient vs angle of attack for NACA0015.

Figure 12: drag coefficient vs angle of attack for NACA0015.

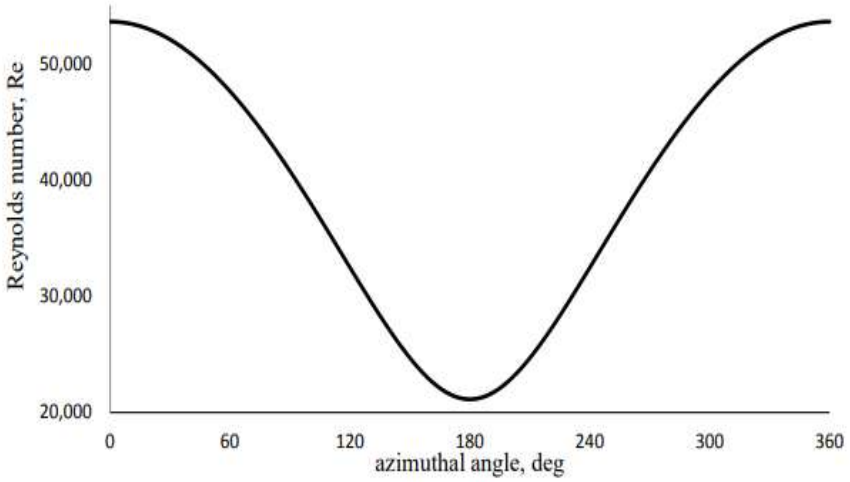

Figure 13: Reynolds number vs azimuthal angle at the equator.

As shown in Figure (13), the Reynolds number reaches the maximum value of 52,000 at (0) deg azimuthal angles and in the upwind zone, the Reynolds number decreases with the increase of azimuthal angle and the converse is also true in the downwind zone.

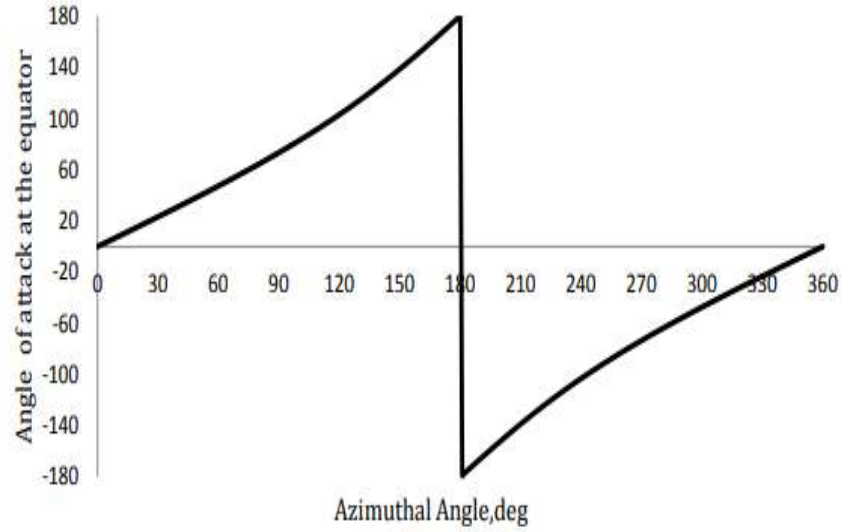

Figure 14: angle of attack as a function of the azimuthal angle at 324 rpm and 0.3 TSR.

The variation in the local angle of attack with blade position (Θ) at the equatorial plane is shown in Figure (14). As can be seen, the blade element theory model predicts the same local angles of attack on the upwind and downwind zones which are symmetrical with respect to Θ =180 deg. Thus, for a tip-speed ratio of TSR=0.34, the upwind local angle of attack α_{max}=180 deg on the downwind face is the same as α_{max}=180 deg.

Prediction data for the tangential-force coefficient for one and two blades at the equator are plotted in Figure (15) for a tip-speed ratio of TSR= 0.34. The variation of this force calculated with blade element theory is similar on both half-cycles of the rotor. The two peak values of C_t occur in the upwind zone of the rotor, about Θ = 30 deg and Θ = 150 deg and in the downwind zone the two peaks of C_t occur, about Θ = 210 deg and Θ =330 deg.

The comparisons between the experimental [9] and the calculations using the blade element theory are shown in figures (16) and (17) for the torque and power coefficient. Figure (16) shows that the experimental are less than the predictions in most of the relative rotor positions, especially in the negative zones and the experimental are greater than the predictions in the range of 90 deg to 120 deg and 230 deg to 240 deg.

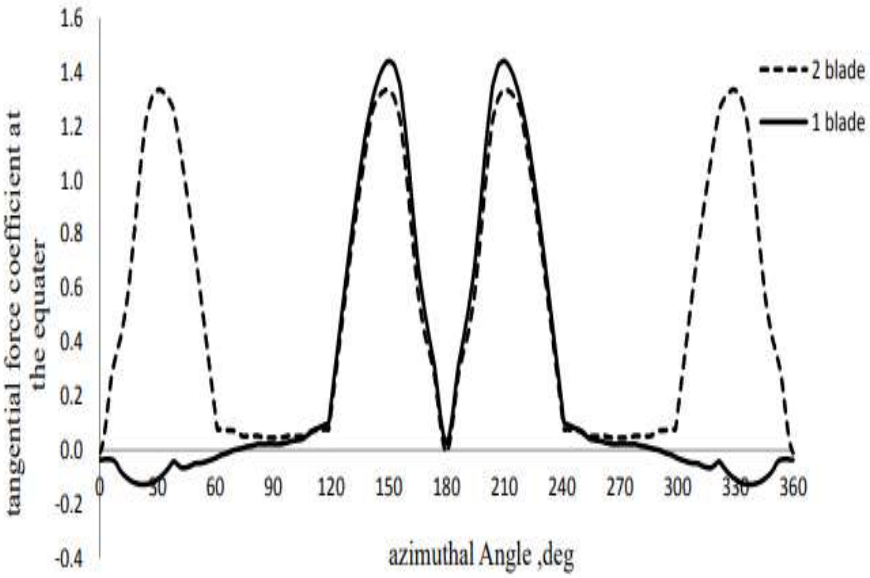

Figure 15: tangential force at the equator vs azimuthal angle for a one & two-bladed rotor**.**

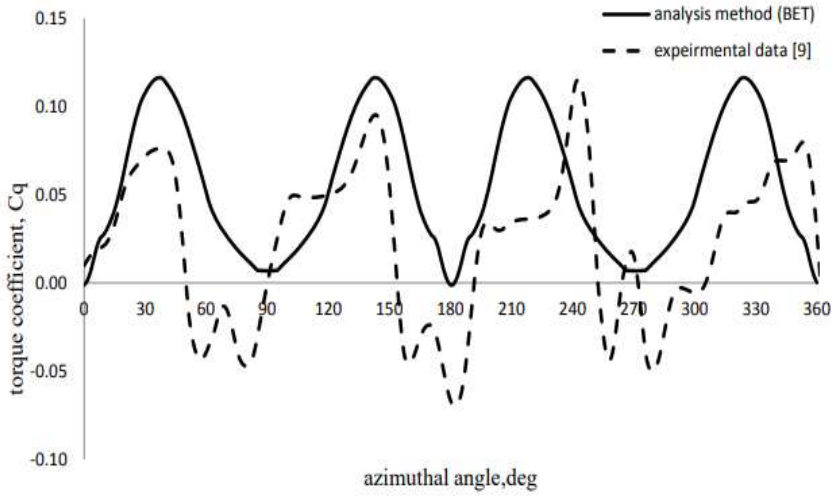

Figure 16: Torque coefficient vs azimuthal angle for a Darrieus, 0.344-meter diameter, a wind turbine with NACA0015 blade section.

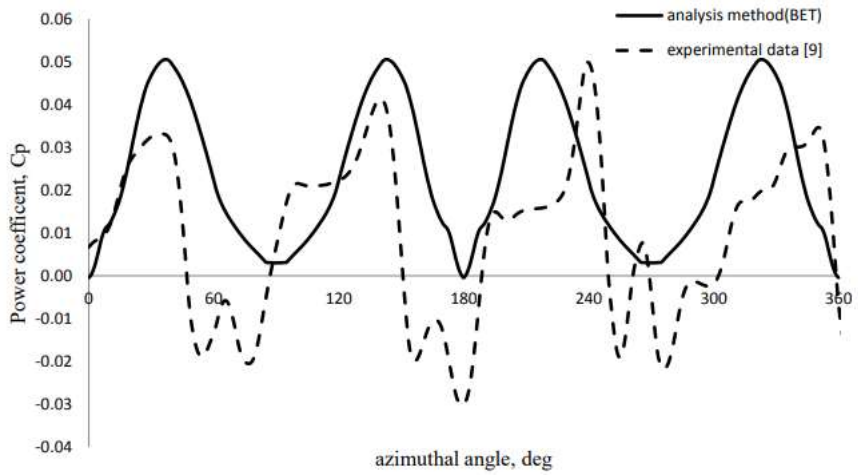

Figure 17: power coefficient versus azimuthal angle for a Darriuse, 0.344-meter diameter, wind turbine with NACA0015 blade section.

Figure (17) shows that the highest performance (C_P of 0.05) was obtained with the two-blade configuration at the rotational speed of 324 rpm. This compares to a maximum of 0.048 obtained with the two-blade configuration during the field test by: Barber. H. [9].

Conclusion

In conclusion, the study provides a comprehensive analysis of the aerodynamics of Vertical Axis Wind Turbines (VAWTs) using the Blade Element Theory (BET). This approach, due to its simplicity and ease of implementation, is widely adopted in wind turbine performance analysis and forms the foundation for many wind turbine design codes. The BET method allows for a more accurate representation of the turbine's behavior compared to the basic actuator disk model. By dividing the blade into independent elements, the induced velocity at each element can be determined, enabling the calculation of aerodynamic forces using lift and drag coefficients derived from empirical wind tunnel tests. This methodology enhances the understanding of VAWT performance, contributing valuable insights for turbine design and optimization.

Acknowledgments

The authors gratefully acknowledge the support provided by the Libyan Center For Land and Marine Environmental Research.

References

[1] DOE (US Department of Energy) News, “http://www.doe.gov/news/6253.htm”, as accurate of August 14, 2008.

[2] Molenaar, D. P., and Dijkstra, S., “State-of-the-art Wind Turbine Design Codes: Main Features Overview for Cost-Effective Generation”, Contract NAS2-11665, Muadyne Report 83-2-3, John Wiley and Sons, 2006.

[3] Ragheb, M., “Vertical Axis Wind Turbines”, August 2011

[4] Chang, L., “Advanced Topics in Environmental Engineering -Wind Power,” Ch 4. University of New Brunswick. Retrieved from http://www.ece.unb.ca/powering /courses/EE6693/index.html in October 2005.

[5] Sheldahl, R. E. and Klimas, P.C., Aerodynamic Characteristics of Seven Airfoil Through 180 Degrees Angle of Attack for Use in Aerodynamic Analysis of Vertical Axis Wind Turbines, SAND80-2114, March 1981, Sandia National laboratories, Albuquerque, New Mexico.

[6] Hansen, M. O. L., “Aerodynamics of wind Turbines”, Vames Et James (Science Publisher) Ltd., London, UK, 2000.

[7] Templin, R. J.,”Aerodynamic Performance Theory for the NRC Vertical –Axis Wind Turbine,” N. A. E. Report LTR-LA-160, Jun1974.

[8] Glauert, H., The Element of Airfoil and Airscrew Theory, 2nd Edition., Cambridge University Press,1948.
[9] Barber, H., "Carleton University VAWT Wind Tunnel Test Model", November 2012.